




The mechanism of egg production improvement in laying hens before and after molting revealed by transcriptome and metabolome integration

Mengqing Sun^a, Hailing Wang^a, Xinyu Zhu^a, Xiaohan Zhang^a, Yahong Min^{a,b}, Ming Ge^{a,b}, Xiaowen Jiang^{a,b}, Wenhui Yu^{a,b,c,*} 

^a College of Veterinary Medicine, Northeast Agricultural University, Harbin 150030, PR China

^b Institution of Traditional Chinese Veterinary Medicine, Northeast Agricultural University, Harbin 150030, PR China

^c Key Laboratory of the Provincial Education Department of Heilongjiang for Pathological Anatomical Medicine and Animal Pathogenesis, Harbin 150030, PR China

ARTICLE INFO

Keywords:

Forced molting
Follicular development
PI3K-AKT signaling pathway
Serum metabolism

ABSTRACT

The objective of this research was to examine the effects and underlying mechanisms of forced molting on the laying rate of hens. A total of ninety 500-day-old laying hens were randomly assigned to three groups: a control group (CK), a starvation group (SG), and a recovery group (RG). The study evaluated follicular development in hens and measured the expression levels of antioxidant, lipid, and inflammatory factors in their serum. Additionally, transcriptomic and metabolomic analyses were performed to assess the effects of forced molting on gene expression and metabolic profiles in hens. The findings indicated that forced molting led to an increase of laying rates, a reduction in follicular closure, and a significant rise in the levels of antioxidant enzymes such as GSH, CAT, and SOD, alongside a decrease in MDA levels. Furthermore, there were significant reductions in the blood lipid levels of LDL, HDL, TC, and TG. Additionally, there were notable differences in the inflammatory markers TNF- α , IL-1, and IL-6. The transcriptomic and metabolomic data revealed that forced molting influenced the activation of the PI3K-AKT and mTOR signaling pathways, affecting fatty acid metabolism in laying hens and modulating the expression of associated genes. In conclusion, this study demonstrates that forced molting is an effective strategy for enhancing the laying rate of hens. Furthermore, it provides a valuable theoretical framework for advancing breeding practices aimed at improving egg production.

Introduction

In the field of layer breeding, the rate of egg production is a crucial metric for assessing breeding efficiency and ensuring a stable market supply (Wang et al., 2022). As the global population continues to grow and concerns about food security intensify, the demand for egg products is increasing (Kumar, et al., 2022). Consequently, the pursuit of effective and sustainable strategies to enhance egg production rates has become a central focus in both research and practice within the poultry farming industry (Li, et al., 2022; Qiang, et al., 2023).

The natural molting process in laying hens is an adaptive physiological mechanism that has evolved over time (Mishra, et al., 2022). This phenomenon is triggered by a combination of internal and external factors, including seasonal variations, changes in photoperiod, advancing age, and fluctuations in hormone levels (Berry, 2003; Wideltz, et al., 2019). During the natural molting phase, the physiological

resources of laying hens are primarily allocated to feather regeneration, resulting in a significant decrease in egg production or a complete cessation of it (Contina, et al., 2023; Herremans, 1988). The duration of the molting process can vary significantly. This timing is influenced by factors such as breed, age, health status, and environmental conditions (Jenni, et al., 2020; Korver, 2023; Zimova, et al., 2018). For the laying hen industry, the significant decrease in egg production associated with natural molting leads to direct economic losses and threatens the sustained availability of egg products in the market (Zhang, et al., 2022b).

The advent and evolution of forced molting aim to mitigate the disadvantages associated with natural molting by actively intervening in the physiological cycles of poultry to enhance egg production rates (Huo, et al., 2020). This approach involves inducing a specific physiological stress state in poultry by precisely regulating key factors such as the feeding environment, nutrient composition, light exposure, and water supply (Attia, et al., 1994; Bozkurt, et al., 2016). The objective is

* Corresponding author: Wenhui Yu, Department of Veterinary Medicine, Northeast Agricultural University, No.600 Changjiang Road, 150006 Harbin, Heilongjiang Province, China.

E-mail address: yuwenhui@neau.edu.cn (W. Yu).

<https://doi.org/10.1016/j.psj.2025.105125>

Received 5 January 2025; Accepted 1 April 2025

Available online 2 April 2025

0032-5791/© 2025 The Authors. Published by Elsevier Inc. on behalf of Poultry Science Association Inc. This is an open access article under the CC BY-NC-ND license (<http://creativecommons.org/licenses/by-nc-nd/4.0/>).

to prompt poultry to enter the molting process quickly and to facilitate the renewal of feathers and the reorganization of physiological functions in a planned and systematic manner within a relatively short timeframe (Elsagheer, et al., 2024). However, the current literature on forced molting remains limited, and the mechanisms by which forced molting influences the growth and development of laying hens, as well as promotes follicle re-maturation, have yet to be fully elucidated. This study aims to investigate the follicular transcriptome and serum metabolome by evaluating follicle development, antioxidant levels, and lipid profiles in laying hens before and after the implementation of forced molting. This research explores the potential relationships between forced molting, gene expression, and metabolite profiles.

Materials and methods

Ethics statement

The trial received approval from the Institutional Animal Care and Use Committee at Northeast Agricultural University (approval number: NEAUEC20240394). All animal experiments adhered to the ARRIVE guidelines.

Animals, diets, and management

A total of 90 Hy-Line Brown laying hens, each 500 days old, were procured from Harbin Hefeng Animal Husbandry Co., Ltd. Following a one-week acclimatization period in the poultry breeding laboratory at Northeast Agricultural University, the hens were randomly assigned to three experimental groups: a control group (CK), a reduced diet starvation group (SG), and a recovery group (RG), with 30 hens assigned to each group. Each group was further subdivided into three parallel replicates. The hens were individually housed in cages measuring 400 mm x 380 mm x 360 mm. Before the trial began, the hens in the SG and RG were gradually subjected to reduced feed supply, and the light duration was decreased by 2 h each day. At the commencement of the trial, each hen in the CK group received 100 g of feed, while hens in the SG and RG groups were provided with 20 g of feed twice daily at 9 AM and 5 PM (refer to Table 1 for feed formulations). During the 12-day enforced molting period, the lighting was limited to 8 h per day, and the ambient

temperature was maintained between 26 and 28 °C. Following this period, the RG group’s feed intake was reinstated, and the duration of light exposure was gradually increased by 2 h per day until it reached a total of 16 h, again lasting 16 days. Throughout the entire experimental duration of 28 days, the indoor temperature was consistently regulated between 23 and 25 °C, with humidity levels maintained between 60 % - 70 % (refer to Supplementary Materials 1 S-Table 1 for specific details on the molting process).

Tissue sample collection and processing

Throughout the testing period, daily records were kept of the number of eggs produced, and the weights of the laying hens were documented. On day 0 (control group), day 12 (SG), and day 28 (RG), six hens were randomly selected from each group. A 2 mL blood sample was collected from the wing venous plexus, and a portion of the serum was subsequently isolated. The hens were subsequently euthanized using carbon dioxide. Following this, the ovaries were excised and dissected, and the follicles were documented. These tissues were preserved in 4 % paraformaldehyde, while the remainder was stored at -80 °C for future analysis.

Histopathological analysis

The freshly collected ovaries were fixed using 4 % paraformaldehyde and subsequently dehydrated through a series of ethanol gradients (75 %, 80 %, 90 %, 95 %, and 100 %). Subsequently, the samples were cleared with xylene, embedded in paraffin wax, and sectioned into 4 μm slices. These slices were then stained with hematoxylin and eosin (H&E) and subsequently mounted using neutral gum. The histopathological alterations in the ovaries were examined using an XD30A-RFL microscope (Zhejiang Sunshine Optical Technology Co., Ltd., China).

Serum levels of antioxidant, lipid and inflammatory factors

The serum, which had been stored at -80 °C, was thawed at 37 °C for one h. The expression levels of antioxidant-related GAT in the serum were evaluated according to the protocols provided in the kits for GSH (A005-1-2), CAT (A007-1-1), MDA (A003-1-2), SOD (A001-3-2), and T-AOC (A015-2-1) from Nanjing Jiancheng Bioengineering Institute. Additionally, the serum lipid content was assessed using LDL (60736ES59), HDL (60737ES59), TC (60723ES60), and TG (53563ES03) kits provided by Yisheng Biotechnology (Shanghai) Co., Ltd. The levels of inflammatory cytokines in the serum were measured using TNF-α (ml002790), IL-1 (ml023407), and IL-6 (ml023415) kits obtained from Shanghai Enzyme-Linked Biotechnology Co., Ltd.

Transcriptome sequencing of ovarian tissue

Ovarian tissue stored at -80 °C was extracted and subsequently thawed on ice. From each group, three samples were obtained, with 0.2 g of tissue extracted for analysis. Total RNA was isolated using TRIzol (R0016, Biyuntian Biotechnology Co., Ltd., Shanghai, China). The purity and concentration of the RNA were assessed using a NanoDrop 2000 spectrophotometer. The integrity of the RNA was assessed using the Agilent 2100/LabChip GX system (Agilent Technologies Co., Ltd., China). Eukaryotic mRNA was enriched using magnetic beads coated with Oligo(dT), followed by random fragmentation using Fragmentation Buffer (11377ES96, Yisheng Biotechnology Co., Ltd., Shanghai, China). The first strand of complementary DNA (cDNA) was synthesized, followed by the synthesis of the second strand, resulting in purified cDNA. The purified double-stranded cDNA underwent end-repair, the addition of an A-tail, and the ligation of sequencing adapters. Fragment size selection was performed using AMPure XP beads, and the cDNA library was generated through polymerase chain reaction (PCR) enrichment. Initial quantification was performed using a Qubit 3.0 fluorometer,

Table 1
Composition and nutrient content of the diets.

Items	No choline chloride basal diet
Ingredients, %	
Corn	60
Soybean meal (46 % crude protein)	20
Wheat bran	5
Limestone	9
Monocalcium phosphate	1.5
DL-Methionine	0.15
L-Lysine HCL	0.2
Premix	1.0
Total Calculated nutrient composition, %	100.0
Metabolizable energy, MJ/kg	11.7
Crude protein	16.5
Calcium	3.5
Total phosphorus	0.7
Available phosphorus	11.28
Lysine	0.8
Methionine + Cysteine	0.7

Note: Vitamin A, 10,000 IU/kg; Vitamin D₃, 2,000 IU/kg; Vitamin E, 30 mg/kg; Vitamin K₃, 2 mg/kg; Vitamin B₁ (Thiamine), 1.8 mg/kg; Vitamin B₂ (Riboflavin), 6 mg/kg; Vitamin B₃ (Niacin), 20 mg/kg; Vitamin B₅ (Calcium Pantothenate), 12 mg/kg; Vitamin B₆ (Pyridoxine), 3 mg/kg; Vitamin B₁₂, 0.02 mg/kg; Folic Acid, 1 mg/kg; Biotin, 0.1 mg/kg; Choline, 500 mg/kg; Iron (Ferrous Sulfate), 80 mg/kg; Zinc (Zinc Oxide), 60 mg/kg; Manganese (Manganese Sulfate), 80 mg/kg; Copper (Copper Sulfate), 8 mg/kg; Iodine (Potassium Iodide), 0.35 mg/kg; Selenium (Sodium Selenite), 0.15 mg/kg.

aiming for a target concentration greater than 1 ng/ μ L. The Qsep400 high-throughput analysis system was utilized to evaluate the inserted fragments of the library. Once the inserted fragments met the required specifications, the effective concentration of the library was accurately quantified using the quantitative polymerase chain reaction (Q-PCR) method, ensuring it exceeded 2 nM. Following successful quality control, the library underwent high-throughput sequencing in PE150 mode. Bioinformatics analysis of the resulting data, which included differential expression analysis as well as gene function annotation and enrichment, was performed using the BMKCloud platform (<https://international.biocloud.net/>; www.biocloud.net). The dynamics of the ovaries of molting birds are closely related to the reproductive cycle, molting stages, and hormonal fluctuations. To control the time-dependent variables, adopting the following strategies: The sampling time is strictly matched to a specific period of the growth stage of primary follicles. The molting process is evaluated according to the Pin Feather Index (PFI) and the microscopic structure of feather buds. Samples are only collected during the Inter-molt stage to avoid the interference of molting-related metabolic pathways. All samples are collected within a fixed time window (8:00 a.m.) to eliminate the influence of diurnal fluctuations in gene expression. The excised tissues are immersed in liquid nitrogen within 2 mins to avoid gene expression changes induced by ischemia and hypoxia. All samples are from age-matched individuals ($n = 3$) of the same strain and under the same rearing conditions (lighting, temperature, and feed). The RNA-seq data were analyzed using the limma package. The significance thresholds were set as \log_2 (fold change) ≥ 1 and adjusted p-value (FDR) < 0.05 . The screening results were visualized using a volcano plot, and the significantly differentially expressed genes (DEGs) were retained. GO and KEGG enrichment analyses were performed based on the DAVID database, with the species background set as *Gallus gallus*. The protein-protein interaction network was analyzed using the STRING database and visualized using Cytoscape V3.7.

Western blot and immunohistochemistry assay

A total of 0.1 g of ovarian tissue was collected from each experimental group. The tissue was homogenized at 12,000 rpm and a temperature of 4 °C for 1 min, followed by centrifugation at the same speed and temperature for 10 min to collect the supernatant. The supernatant was then dissolved in RIPA buffer containing protease and phosphatase inhibitors to enhance protein extraction. The protein concentration was quantified using a BCA assay kit (PC0020, Solarbio Biotechnology Co., Ltd., Beijing, China). Following this, the samples were separated using SDS-PAGE and subsequently transferred electrically to a methanol-pretreated PVDF membrane. The membrane was blocked with 5 % BSA for 2 h and then incubated overnight with a primary antibody at the dilution ratios specified in S-Table 2. Subsequently, the membranes were incubated with a goat anti-rabbit secondary antibody diluted to 1:10,000. The chemiluminescent signal was generated using an electrochemiluminescence (ECL) solution and visualized with a chemiluminescence detection system (5200 Multi, Tianneng Life Science Co., Ltd., Shanghai, China).

In parallel, ovarian tissue sections were treated with an EDTA antigen extraction solution, subjected to high-temperature heating and boiling, and then allowed to cool to room temperature. The sections were subsequently washed with phosphate-buffered saline (PBS) and then treated with a diluted Ki67 primary antibody (1:500), which was incubated at 4 °C for 6 h. For secondary antibody incubation, the sections were washed with phosphate-buffered saline (PBS) and then incubated in the dark with an Alexa Fluor 488-conjugated secondary antibody (diluted 1:500) for 1 h. The nuclei were stained with DAPI (1:1000) for 10 mins. Finally, the sections were mounted with using anti-fade mounting medium, observed under a fluorescence microscope, and photographed. The band density and fluorescence intensity were assessed using ImageJ software, after which the relative expression

levels of the protein were determined.

Serum metabolome

A pipettor was used to accurately extract 100 μ L of serum from each experimental group, followed by the addition of 500 μ L of an extraction solution containing an internal standard. The solution had a methanol to acetonitrile volume ratio of 1:1 and an internal standard concentration of 20 mg/L. The mixture was then swirled and thoroughly mixed for 30 s, subjected to ultrasonic treatment for 10 mins at 4 °C. Subsequently, 120 μ L of the supernatant from each group was transferred into 2 mL injection vials. The analysis was conducted using ultra-high-performance liquid chromatography (Acquity I-Class PLUS, Waters Technology Co., Ltd., Shanghai, China) coupled with a high-resolution mass spectrometer (Xevo G2-XS QTOF, Waters Technology Co., Ltd., Shanghai, China). Data acquisition was conducted using a 1.8 μ m, 2.1 \times 100 mm column (Acquity UPLC HSS T3, Waters Technology Co., Ltd., Shanghai, China). The mobile phase comprised a 0.1 % formic acid aqueous solution (referred to as mobile phase A) and 0.1 % acetonitrile (referred to as mobile phase B), following a gradient elution procedure as outlined in S-Table 1. The electrospray ionization (ESI) source parameters were configured with a capillary voltage of 2500 V for positive ion mode and -2000 V for negative ion mode, accompanied by a cone-hole voltage of 30 V. The ion source temperature was maintained at 100 °C, while the desolvation temperature was set to 500 °C. The air flow rate was established at 50 L/h and the desolvation gas flow rate was set to 800 L/h. The mass-to-charge (m/z) collection range was established between 50 and 1200. Following data collection, the original data obtained through MassLynx V4.2 were processed using Progenesis QI software, which included peak extraction and alignment. The identification of metabolites was performed using the online METLIN database, a public resource, as well as a self-constructed database within Progenesis QI software, in conjunction with theoretical fragment identification. Data analysis was conducted using the R programming language (version 3.6.1) along with a custom-written script. This analysis included principal component analysis, heat map generation, and orthogonal partial least squares discriminant analysis (OPLS-DA). One-way ANOVA on the metabolomic data obtained from serum detection based on their raw intensities respectively, and we also supplemented this information in the methodology section. Ultimately, the differential gene expression data were integrated with the ten metabolites that displayed the most significant differences among the various sample groups for further analysis.

Result

Forced molting improves egg production and reconstructs ovarian function

After a 28-day forced molting period, a reduction in the body weight of laying hens was observed, with a 27.6 % decrease recorded on day 12 (see Fig. 1A). This weight loss has reached the threshold for time-restricted feeding (Alodan et al., 1999). Concurrently, the laying rate decreased from 60 % on the first day to 0 % by day 7. However, after molting, the laying rate rebounded to 95.35 % by day 28 (see Fig. 1B), indicating that the hens entered a peak laying phase. The development of the ovaries is illustrated in Figs 1C-E. During the early stages of molting, the control group (CK) displayed multiple follicles at various developmental stages, characterized by atresia, degeneration, and a sparse tissue structure. By day 12, the number of follicles in the starvation group (SG) had significantly decreased, with the majority exhibiting atresia and degeneration. Conversely, by day 28, the recovery group (RG) exhibited an increase in the number of primary follicles within the ovarian tissue, accompanied by a denser overall tissue structure. The findings indicate that it is feasible to reduce food consumption to facilitate molting and enhance the rate of egg production.

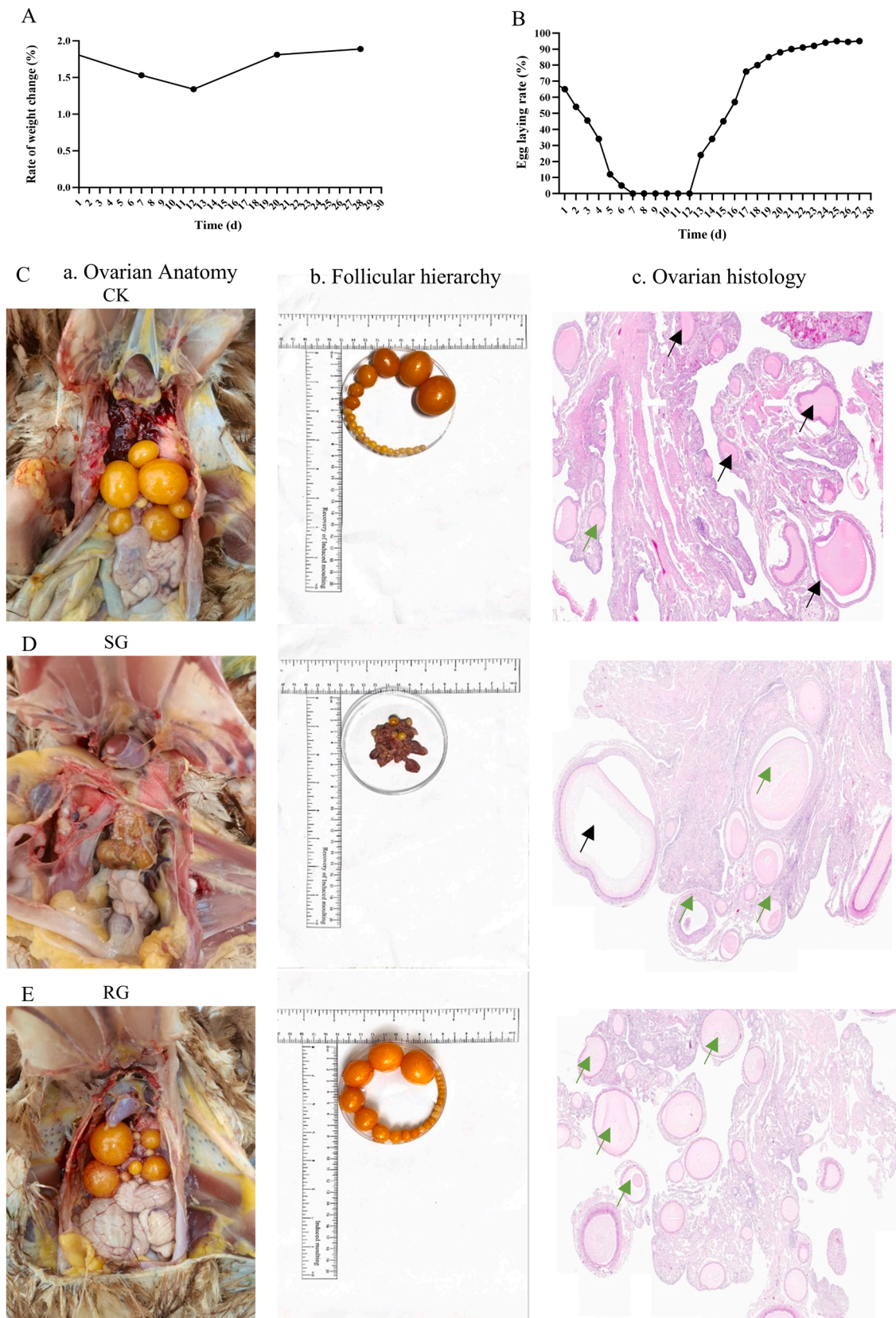


Fig. 1. presents clinical observations related to the implementation of forced molting as a strategy to enhance the rate of egg production. A, the weight trajectory of laying hens; A total of 90 Hy-Line Brown laying hens were used for sampling. B, the laying rate over time; A total of 90 Hy-Line Brown laying hens were used for sampling. C-E, Autopsy findings of the laying hens, including the quantification of follicles and histological examination of the ovaries. Black arrows denote atretic follicles, while red arrows signify follicles exhibiting normal developmental progression.

Effects of forced molting on antioxidant, lipid and inflammation of laying hens

The serum levels of oxidative stress markers, lipid profiles, and inflammatory factors in laying hens during the molting phase are depicted

in Fig. 2. A comparison between the SG group and the CK group revealed a significant reduction ($P < 0.05$) in the levels of GSH, CAT, SOD, and T-AOC in the SG group, along with a notable increase ($P < 0.05$) in MDA levels. Furthermore, when comparing the SG group to the RG group, MDA levels were significantly lower ($P < 0.05$) in the RG group.

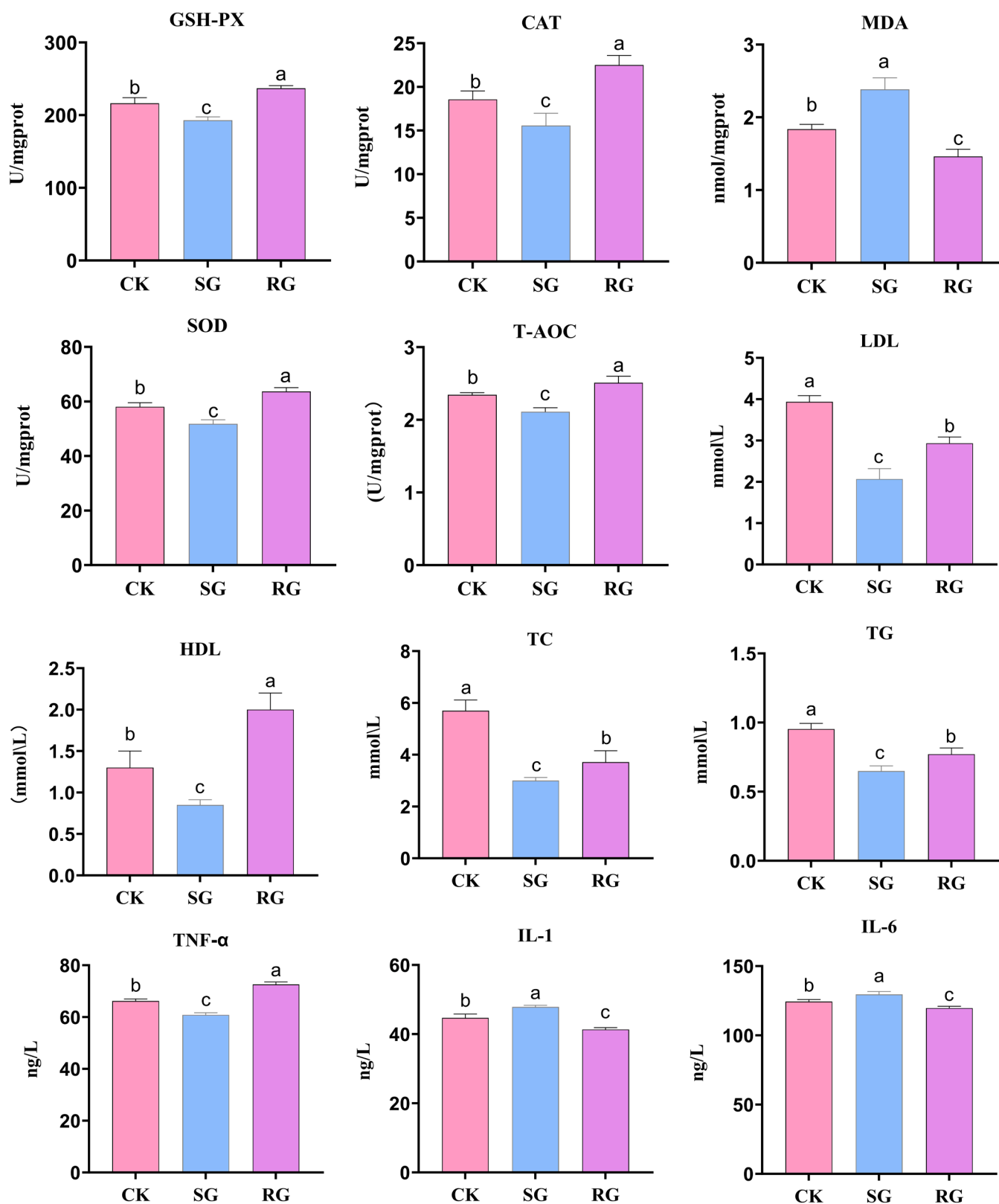


Fig. 2. Effects of forced molting on serum oxidative stress, blood lipids and inflammatory factors of laying hens (a, b, c indicated significant differences $P < 0.05$).

Following molting, the antioxidant indices mentioned earlier in the RG group demonstrated a significant upward trend, with differences achieving statistical significance ($P < 0.01$). Additionally, compared to the CK group, the SG group exhibited a significant decrease ($P < 0.05$) in LDL, HDL, total TC, and TG, these lipid parameters showed a significant recovery trend following molting in the RG group ($P < 0.01$). Among the inflammation-related factors, TNF- α was significantly downregulated in the SG group, while the levels of IL-1 and IL-6 were elevated, with restoration observed in the RG group. These findings indicate a strong correlation between forced molting and the oxidative system, lipid metabolism, and inflammatory responses in laying hens.

Transcriptome sequencing of ovaries of laying hens after molting

As indicated in S-Table 3, following the implementation of sequencing quality control measures, a total of 60.13 Gb of clean data were acquired. Furthermore, the proportion of Q30 bases in each sample was at least 96.50 %, providing a solid foundation for subsequent analyses.

The correlation of gene expression levels across samples is a crucial metric for assessing the reproducibility of biological experimental procedures, evaluating the reliability of differentially expressed genes, and facilitating the identification of anomalous samples. As illustrated in Fig. 3A, the correlation coefficients among samples from all groups are below 1, indicating variability among the samples. The results of the Principal Component Analysis (PCA) shown in Fig. 3B (PC1 = 71.6 %, PC2 = 23 %) demonstrate a favorable degree of dispersion among the samples. To visually represent the overlap of differentially expressed genes across the three groups, Fig. 3C illustrates the presence of 48 differentially expressed genes that are common to all groups. Meanwhile, Fig. 3D shows that there are 1,316 differentially expressed genes identified between the CK group and the SG group, which includes 386 up-regulated genes and 930 down-regulated genes. Additionally, there are 983 differentially expressed genes identified between the CK group and the RG group (Fig. 3E), comprising 495 upregulated genes and 488 downregulated genes. The SG group and RG group exhibit 674 differentially expressed genes (Fig. 3F), comprising 388 upregulated and 286 downregulated genes. Furthermore, cluster heat maps were utilized to illustrate the expression patterns of differentially expressed genes across each group. Fig. 3G illustrates the Gene Ontology (GO) enrichment analysis of the shared genes, indicating that the biological processes predominantly include the negative regulation of proteolysis, the positive regulation of phosphorylation, and the positive regulation of protein secretion. The identified cellular components include respiratory chain complexes, oxidoreductase complexes, and respirasomes. The molecular functions are primarily associated with peptidase inhibitor activity and vitamin binding. The KEGG enrichment analysis (Fig. 3H) indicates that the 48 genes mentioned above are significantly enriched in the PI3K-AKT, mTOR, and apoptosis signaling pathways, as well as in several metabolic pathways. A Protein-Protein Interaction (PPI) network was constructed for the 48 differentially expressed genes (Fig. 3I), revealing that mTOR and PI3K are significantly enriched as central proteins within this network (Fig. 3J).

Effects of forced molting on PI3K-AKT and mTOR signaling pathways

To elucidate the changes in ovarian gene function following induced molting, the differentially expressed genes identified within the protein interaction network were quantified as read counts, with the results illustrated in Fig. 4A. Notably, a comparison between the SG group and the CK group revealed significant differences in the expression levels of PI3K, mTOR, AKT, IL-1, and PHAS1 (P-4E-BP1) ($P < 0.05$). Additionally, a gradual recovery of these expression levels was observed in the RG group ($P < 0.01$). Further examination of the Western blot results corroborated these findings (Fig. 4B). The data indicate that forced molting enhances the expression of PI3K, AKT, mTOR, and PHAS1 (P-

4E-BP1) in the ovaries of laying hens, thereby promoting protein phosphorylation. Furthermore, to investigate the proliferation of ovarian cells in greater detail, Ki-67 expression was evaluated using immunofluorescence techniques. As illustrated in Fig. 4C, Ki-67 expression in the SG group was significantly lower than that in the CK group ($P < 0.05$). In contrast, Ki-67 expression in the RG group was significantly elevated compared to the SG group ($P < 0.01$). These findings suggest that forced molting promotes the restoration of ovarian function by activating the PI3K-AKT-mTOR signaling pathway.

Metabolome in serum of laying hens before and after molting

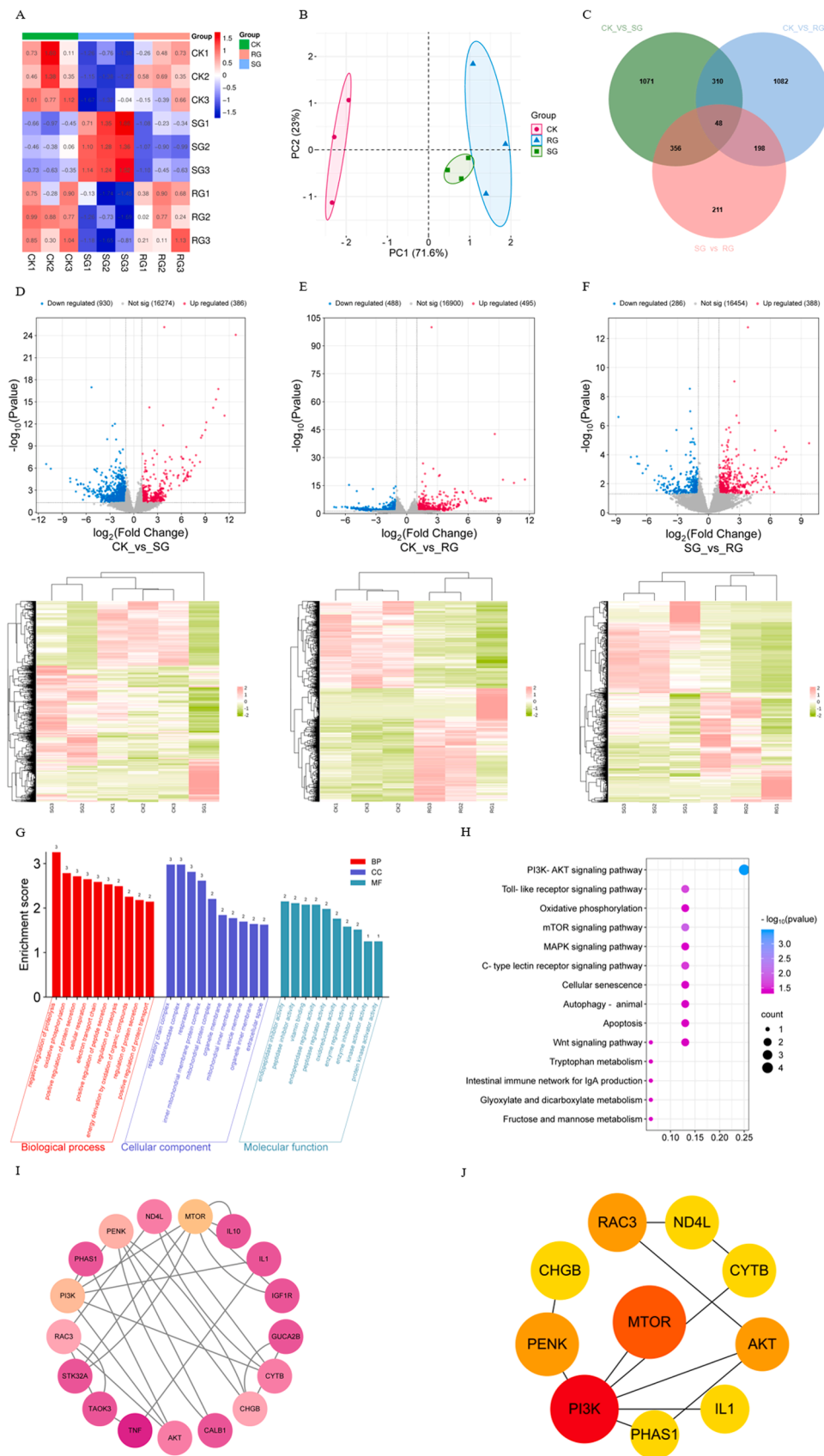
The serum metabolic profiles of laying hens were assessed using non-targeted liquid chromatography-mass spectrometry (LC-MS), and the variations in serum metabolites among different groups were systematically analyzed. Principal Component Analysis (PCA) revealed a statistically significant metabolic difference among the three groups, with PC1 accounting for 72.7 %, PC2 for 13.3 %, and PC3 for 5 % (Fig. 5A). Additionally, the clustering heat map presented in Fig. 5B, which utilizes the Pearson correlation coefficient, illustrates the metabolic differences among the three groups. Fig. 5C further delineates the expression trends of all metabolites across these groups, while Fig. 5D offers a more detailed classification of the metabolites. Notably, fatty acids (including lipids and lipid-like molecules) and carboxylic acids along with their derivatives were the most prevalent, accounting for 17.5 % and 15 % of the total metabolites, respectively. The Venn diagram statistical analysis illustrated in Fig. 5E revealed 116 distinct metabolites across the three groups. In the comparison between the control group (CK) and the treatment group (SG), a total of 543 metabolites were identified, of which 336 were upregulated and 207 were downregulated. In the comparison between CK and RG, a total of 253 metabolites were identified, with 156 being upregulated and 97 downregulated (see Supplementary Materials 2). The comparison between SG and RG identified a total of 827 metabolites, with 418 being up-regulated and 409 down-regulated (Fig. 5F). Radar analysis of the total metabolites (Fig. 5G) highlighted LysoPC (20:3 (5Z, 8Z, 11Z) /0: 0) in terms of its content. Furthermore, KEGG enrichment analysis indicated that these metabolites were predominantly enriched in pathways related to ABC transporters as well as nicotinate and nicotinamide metabolism.

Effects of molting on serum metabolic profile and ovary genes of laying hens

To elucidate the content and trends of differential metabolites across various groups, the top 20 differential metabolites were analyzed using a violin plot based on raw intensity, with the results presented in Fig. 6A. The metabolites LysoPC, Seselin, Argatroban, and Senecioic acid exhibited distinct trends and significant differences among the three groups ($P < 0.05$). To further investigate the relationship between differential metabolites and their associated core genes, a joint analysis was conducted, as illustrated in Fig. 6B. The results indicated that LysoPC and Senecioic acid, among other metabolites, demonstrated a positive correlation with genes such as IL1 and TNF. In contrast, Seselin and Argatroban were positively correlated with genes including AKT and mTOR. These findings suggest that forced molting may influence gene expression by modulating serum metabolite levels.

Discussion

Forced molting is a breeding and management strategy for laying hens that significantly enhances egg production (Zhang, et al., 2021). Forced molting has been recognized as a longstanding practice in the poultry industry, with its origins dating back to the 1960s. Research conducted by Len et al. demonstrated that induced molting allows poultry farmers to effectively regulate the egg production cycle, thereby enhancing both production efficiency and operational sustainability



(caption on next page)

Fig. 3. Transcriptomic analysis of laying hens after forced molting. A, sample expression correlation heat map, the value of each color block on the heat map represents the correlation between the two samples corresponding to the horizontal and vertical axes of the color block, the larger the value, the higher the correlation; B, PCA diagram, different coordinates represent different principal components, percentage represents the contribution value of corresponding principal components to the difference of samples, each point represents a sample, samples in different groups are represented by different colors; C, Venn map of differential gene sets, where the numbers on each region represent the number of genes under the corresponding classification, and overlapping regions represent the number of differential genes shared among related combinations in the region; D-F, differential expression volcano map and clustering heat map, each point in the differential expression volcano map represents a gene, and the horizontal coordinate represents the logarithmic value of the expression difference multiple of a certain gene in two samples; The larger the ordinate value, the more significant the differential expression, and the more reliable the differentially expressed genes. In the figure, blue points represent down-regulated differentially expressed genes, red points represent up-regulated differentially expressed genes, and gray points represent non-differentially expressed genes. In the clustering heat map, the horizontal coordinate represents sample name and sample clustering results, and the vertical coordinate represents differentially expressed genes and gene clustering results. Different columns in the diagram represent different samples, and different rows represent different genes. The color represents the level of gene expression in the sample log10; G, differentially expressed gene GO enrichment histogram, horizontal coordinate for each GO annotated entry. The ordinate is GeneNum, which indicates the number of genes in this entry; H, the KEGG enrichment bubble diagram of differentially expressed genes, in which each circle represents a KEGG pathway, the vertical coordinate represents the pathway name, and the horizontal coordinate represents the Rich factor, representing the ratio of the proportion of genes annotated to a pathway in differential genes to the proportion of genes annotated to this pathway in all genes. The higher the enrichment factor, the more significant the enrichment level of differentially expressed genes in this pathway. I-J, protein interaction network, the higher the gene Degree, the redder the color.

(Len, et al., 1964). Following the forced molting process, the reproductive system of laying hens undergoes a temporary period of rest, during which nutrients within the body are redistributed and accumulated. This physiological adjustment facilitates the storage of sufficient energy and nutrients, ultimately resulting in enhanced laying rates and improved egg quality upon the resumption of egg production (Corrier, et al., 1997). Research has demonstrated that, following forced molting, the laying rate of hens aged 500 days significantly increased, accompanied by an improvement in egg quality (Nishiyama, et al., 2021). Furthermore, this study indicated that the laying rate of hens improved due to the secondary development and maturation of follicles, while the occurrence of atretic follicles decreased. These findings underscore the feasibility of implementing forced molting as a management practice for laying hens. The ovary serves as the primary organ for egg production in laying hens, playing a crucial role in the processes of egg development, maturation, and ovulation (Tang, et al., 2023). These processes are associated with the generation of a substantial quantity of free radicals, including superoxide anions and hydroxyl radicals (Ritsick, et al., 2007). The antioxidant system in the bodies of laying hens, which includes various antioxidant enzymes such as SOD and GSH-Px, effectively neutralizes free radicals and reduces the production of MDA, thereby maintaining oxidative balance within the ovaries (Xing, et al., 2022). When the antioxidant capacity of laying hens is optimal, it can significantly reduce oxidative damage to ovarian tissue cells, thereby preserving their normal structure and function (Gao, et al., 2021). This preservation is essential for the proper development of eggs and the ovulation process, ultimately facilitating increased egg production. The present study revealed that the oxidative stress system in laying hens was adversely affected during the period of dietary reduction, as evidenced by an elevation in MDA levels. Additionally, research conducted by Yan et al. (Yan, et al., 2023) demonstrated that salpingitis induced by bacterial infection also resulted in oxidative stress, which correlated with a decline in egg production, thereby supporting the findings of the current investigation.

LDL cholesterol plays a vital role in transporting cholesterol to peripheral tissues (Borrell-Pages, et al., 2024). In the ovaries of laying hens, LDL facilitates the delivery of cholesterol essential for processes such as ovarian hormone synthesis (Perry, et al., 1984). However, a significant reduction in LDL levels can lead to oxidative stress and the formation of oxidized LDL, which may damage the vascular endothelial cells of the ovaries, instigate inflammation, impair blood supply to the ovaries, and subsequently hinder follicular development and ovulation (Lu, et al., 2011; Wang, et al., 2024; Wu, et al., 2021). Conversely, HDL in the circulatory system surrounding the ovaries facilitates the removal of excess cholesterol. This process helps prevent the excessive accumulation of cholesterol in ovarian tissue, thereby mitigating potential adverse effects on ovarian function (Kim, et al., 2022). Research indicates that elevated levels of HDL may provide protective benefits for

ovarian health and support normal egg production in laying hens (Lim and Ryu, 2022). Total cholesterol is a crucial precursor for steroid hormone synthesis, as it is essential for the production of sex hormones, such as estrogen, in the ovaries of laying hens (Tian, et al., 2019). Maintaining moderate levels of total cholesterol is essential for supporting normal hormone synthesis, which, in turn, promotes follicular development and maturation (Yang, et al., 2022). Conversely, excessively low total cholesterol levels can result in inadequate estrogen production, adversely affecting follicular growth and diminishing the laying performance of hens (Gu, et al., 2021). Additionally, triglycerides play a crucial role in supplying energy to the body. Maintaining adequate triglyceride levels is essential to ensure that ovarian cells receive sufficient energy to support normal ovarian tissue function (Liu, et al., 2024). However, excessively high triglyceride levels may impair the protective function of fat for the ovaries, potentially resulting in ovarian atrophy and adversely affecting ovarian function (Hu, et al., 2024). The findings of this study indicate that the lipid content in laying hens experienced a significant reduction following the forced molting process. Subsequently, during the recovery phase, there was a gradual increase in the serum lipid levels of the hens, which may be closely associated with the observed rise in egg production levels. TNF- α is integral to the immune response and inflammatory processes (Chen and Goeddel, 2002). Research indicates that stress induced by forced molting may lead to a reduction in TNF expression, potentially mitigating apoptotic responses within the organism's cells. This reduction could otherwise increase susceptibility to infection or injury (Sundaresan, et al., 2007; Zhang, et al., 2022a). IL-1 exhibits pro-inflammatory and immunomodulatory properties that activate immune cells and enhance inflammatory responses, thereby strengthening the body's immune defenses (Schmitz, et al., 2005). IL-6 is a multifunctional cytokine that plays a critical role in immune regulation, inflammatory responses, and hematopoiesis (Wein, et al., 2020). The process of forced molting may induce variations in IL-6 levels (Nii, et al., 2011). A moderate increase in IL-6 may facilitate the adaptation of laying hens to the physiological changes associated with molting; however, excessive elevations could lead to detrimental effects, including tissue damage and immune dysfunction (Sundaresan, et al., 2008). The present study observed a decrease in TNF- α release during the molting phase of laying hens, accompanied by a significant increase in the expression levels of IL-1 and IL-6, corroborating findings from previous research. Furthermore, these indices exhibited a gradual recovery in the later stages of molting, coinciding with a reduction in the occurrence of follicular atresia, as evidenced by pathological examinations.

Alterations in the ovarian transcriptome significantly influence the egg-laying performance of hens (Sun, et al., 2021). Following a successful forced molting process, the ovarian functionality of laying hens can be restored and enhanced, resulting in an extended subsequent laying cycle and potential improvements in laying rates (Xiang, et al.,

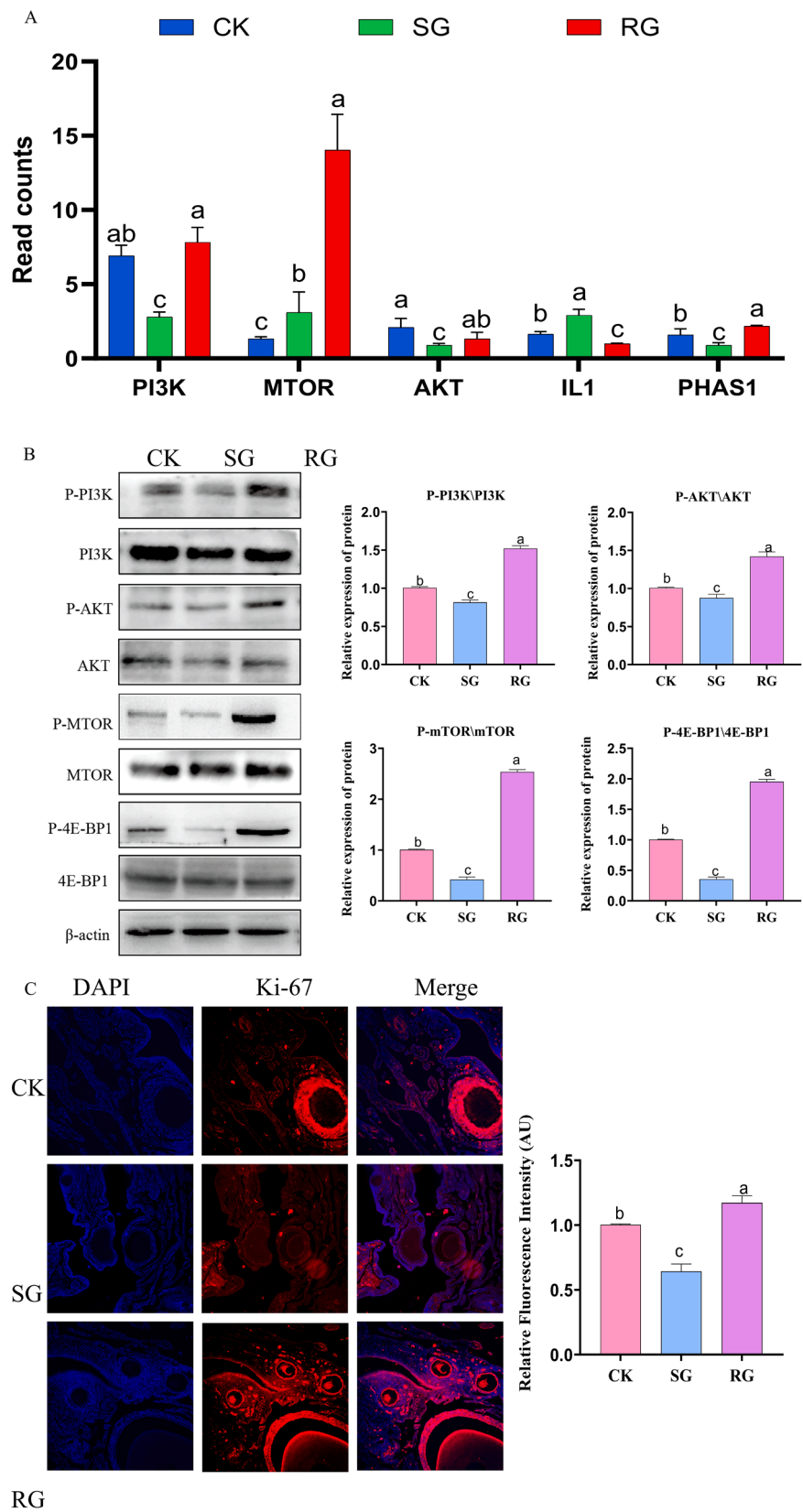
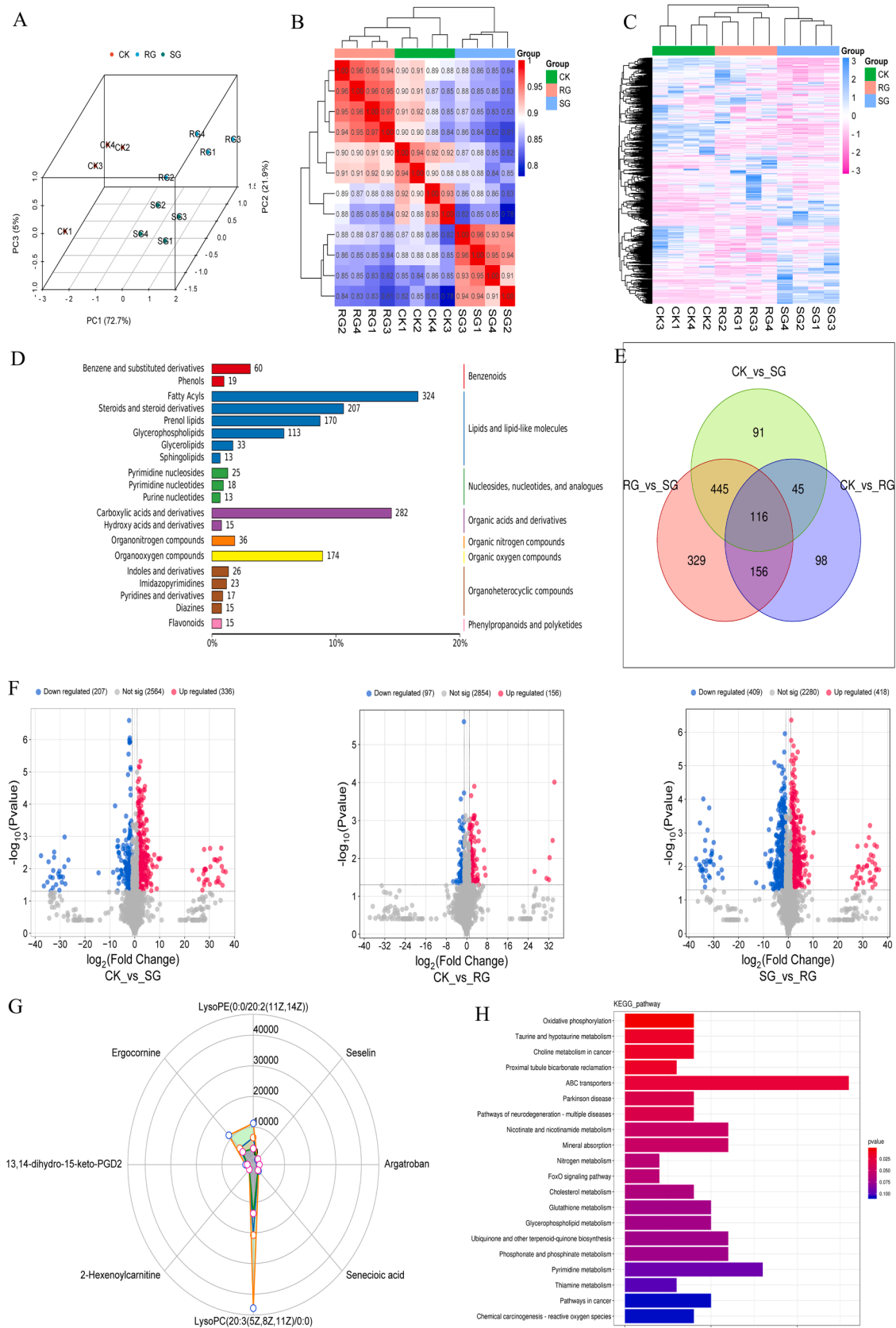


Fig. 4. Expression levels of PI3K-AKT and mTOR pathways in ovary of laying hens before and after molting. A, Read Counts in transcriptome sequencing, with different colors representing different groups (a, b, c representing significant differences $P < 0.05$); B, Western-blot analysis of protein expression levels (a, b, c represented significant difference $P < 0.05$); C, expression of Ki-67 in ovarian tissue, (a, b, c represents significant difference $P < 0.05$).



(caption on next page)

Fig. 5. Serum metabolic profile of laying hens before and after molting. A, 3D map of PCA analysis; B, Using the clustering heat map with Pearson coefficient statistical analysis, the closer the number is to 1, the higher the similarity between samples; C, the overall hierarchical clustering analysis heat map of all samples, the abscissa represents different sample groups, the ordinate represents all metabolites, the color blocks at different positions represent the relative expression of metabolites at corresponding positions, red indicates high metabolite content, blue indicates low metabolite content; D, Histogram of statistical analysis of metabolites, with different colors representing the classification of different metabolites; E, metabolites have Venn diagram, different colors represent different groups; F, volcanic maps of differentiated metabolites in different groups, red represents up-regulated metabolites, blue represents down-regulated metabolites, and gray represents non-significant differentiated metabolites; G, differential metabolite distribution radar map, grid lines represent log2FC, shadows consist of log2FC lines for each metabolite; H, KEGG enrichment analysis of differential metabolites, the darker the color indicates the more significant the difference, and the longer the column indicates the more enrichment of differential metabolites.

2022). This investigation revealed significant changes in the ovarian gene expression of laying hens before and after molting, primarily linked to alterations in the PI3K-AKT-mTOR signaling pathway. The PI3K-AKT signaling pathway is essential for cellular survival, proliferation, and metabolism (Cheng, et al., 2020). Research indicates that this pathway may be inhibited during the initial stages of molting due to changes in nutritional and hormonal levels, including a reduction in PI3K activity. This reduction subsequently decreases the phosphorylation of Akt, thereby affecting cell survival and proliferation (Li and Wang, 2017). Following the improvement of environmental and nutritional conditions, the activity of the PI3K-Akt signaling pathway gradually recovers. An increase in Akt phosphorylation enhances the survival of ovarian cells by inhibiting the pro-apoptotic protein Bad (She, et al., 2005). Concurrently, Akt regulates the expression of genes associated with cellular metabolism, facilitating nutrient uptake and utilization, thereby creating favorable conditions for follicular regeneration (Zhu, et al., 2021). mTOR, a serine/threonine protein kinase, integrates various signals, including nutrients and growth factors, to regulate cell growth and metabolism (Ragupathi, et al., 2024). Evidence indicates that the activity of the mTOR signaling pathway in laying hens decreases during the molting phase due to nutritional constraints. This reduction leads to decreased protein synthesis and inhibits cell growth and proliferation (Heryanto, et al., 1997). For instance, the phosphorylation of the downstream mTOR target, ribosomal protein S6 kinase (S6K), is reduced, resulting in decreased ribosomal protein synthesis and an overall decline in cellular metabolic activity as a response to nutrient deficiency (Xie, et al., 2018). The development of ovarian follicles, which includes the transition from primary to secondary follicles as well as the selection and maturation of dominant follicles, is characterized by the proliferation of follicular cells (Cheng, et al., 2024). Ki-67 is prominently expressed during the active phase of the ovarian cell cycle and serves as a crucial marker for evaluating cell proliferation status (Briño-Enríquez, et al., 2023). Variations in Ki-67 expression levels can serve as direct indicators of the proliferative activity of follicular cells at various developmental stages. PHAS1 (PHAS1, or phosphorylated ribosomal protein S6 kinase 1) is a protein regulated by the TOR (target of rapamycin) signaling pathway, which responds to a variety of environmental factors, including nutritional status and growth factor signaling within cells (Brunn, et al., 1996). In nutrient-rich environments with adequate growth factors, TOR is activated and phosphorylates PHAS1, thereby facilitating cell proliferation (Roh, et al., 2003). This study observed fluctuations in the PI3K-AKT-mTOR signaling pathway, as well as in the levels of phosphorylated Ki-67 and PHAS1 proteins in the ovaries of laying hens before and after molting. These findings suggest that forced molting can stimulate the expression of Ki-67 and PHAS1 through this signaling pathway, thereby promoting the proliferation of ovarian cells and enhancing egg production.

The impact of forced molting on serum metabolism and reconstitution represents a significant aspect of this phenomenon (Landers, et al., 2008). The present study identified several metabolites involved in this reconstitution process, including LysoPC, Seselin, Argatroban, and Senecioic acid. LysoPC, a crucial product of phospholipid metabolism within cellular membranes, exhibits relatively stable levels in the serum of laying hens (Huang, et al., 2020). Research has shown that LysoPC is a lipid with pro-inflammatory activity, and elevated levels of LysoPC can be observed under various pathophysiological conditions (Ge et al.,

2020). The levels of pro-inflammatory factors such as IL-6 are positively correlated with the levels of LysoPC (Ha et al., 2012). In this study, it was found that the level of LysoPC increased in the SG group. At the same time, the level of IL-6 in the serum of laying hens in the SG group also increased. It is speculated that the elevation of LysoPC in the SG group is caused by the remodeling of ovarian cells in laying hens. In the study conducted by Chen et al. (Len, et al., 1964), it was found that adding probiotics to the diet can also lead to a decrease in LysoPC in the intestinal metabolites of laying hens in the late laying period and alleviate intestinal cell damage. This result is similar to that of this study. During the normal laying phase, LysoPC concentrations play a crucial role in maintaining cellular functions, facilitating the transport of nutrients and hormones, and establishing an optimal internal environment for follicular development and yolk formation (Chen, et al., 2023). Molting stress can disrupt cellular metabolic processes, leading to an imbalance between the degradation and synthesis of phospholipids in cell membranes. To meet energy demands, some phospholipids may be catabolized, resulting in an increase in LysoPC production. Concurrently, nutritional deficiencies may impede the further metabolism of LysoPC, causing its accumulation in the serum (Ruan, et al., 2024). The findings of this study indicate an increase in LysoPC content during the molting phase. This alteration may influence cellular signal transduction mechanisms, particularly those associated with growth factor signaling pathways, thereby impacting the physiological functions of laying hens. Seselin, a natural coumarin-like compound, may play a role in maintaining REDOX balance and immune homeostasis in laying hens, thus providing a stable internal environment conducive to normal physiological activities and supporting the health and reproductive performance of these birds (Surai and Fisinin, 2014). The antioxidant properties of seselin may reduce the accumulation of intracellular reactive oxygen species (ROS) and protect cells from oxidative damage (Chidambaram, et al., 2021); This study observed an increase in serum seselin levels following molting, suggesting its role as an endogenous protective agent in response to oxidative stress and inflammation. Argatroban, a thrombin inhibitor, prevents excessive coagulation, thereby ensuring efficient blood circulation and the transport of nutrients and hormones to various tissues and organs, including reproductive structures such as the ovaries and fallopian tubes, thus supporting the reproductive functions of laying hens (McKeage and Plosker, 2001). The observed increase in argatroban levels post-molting may be associated with functional changes in vascular endothelial cells, which are critical to coagulation and anticoagulation processes. The stress associated with molting may influence the secretion or metabolism of argatroban by these endothelial cells (Zhao, et al., 2022). Senecioic acid, typically present in lower concentrations in the serum of normal laying hens, is an organic acid that may be implicated in fatty acid metabolism (Soares, et al., 2025). This study found that, due to a reduced nutrient intake, laying hens began to utilize their fat reserves for energy, resulting in a significant increase in senecioic acid levels (Greger, et al., 1996). This suggests that senecioic acid may play a role in regulating fat mobilization, promoting the breakdown of triglycerides in adipose tissue, and facilitating the release of fatty acids for energy production. Simultaneously, the correlation analysis revealed a positive association between LysoPC and other metabolites within the PI3K-AKT signaling pathway. This finding may further support the hypothesis that alterations in metabolite levels activate associated pathways, thereby facilitating the

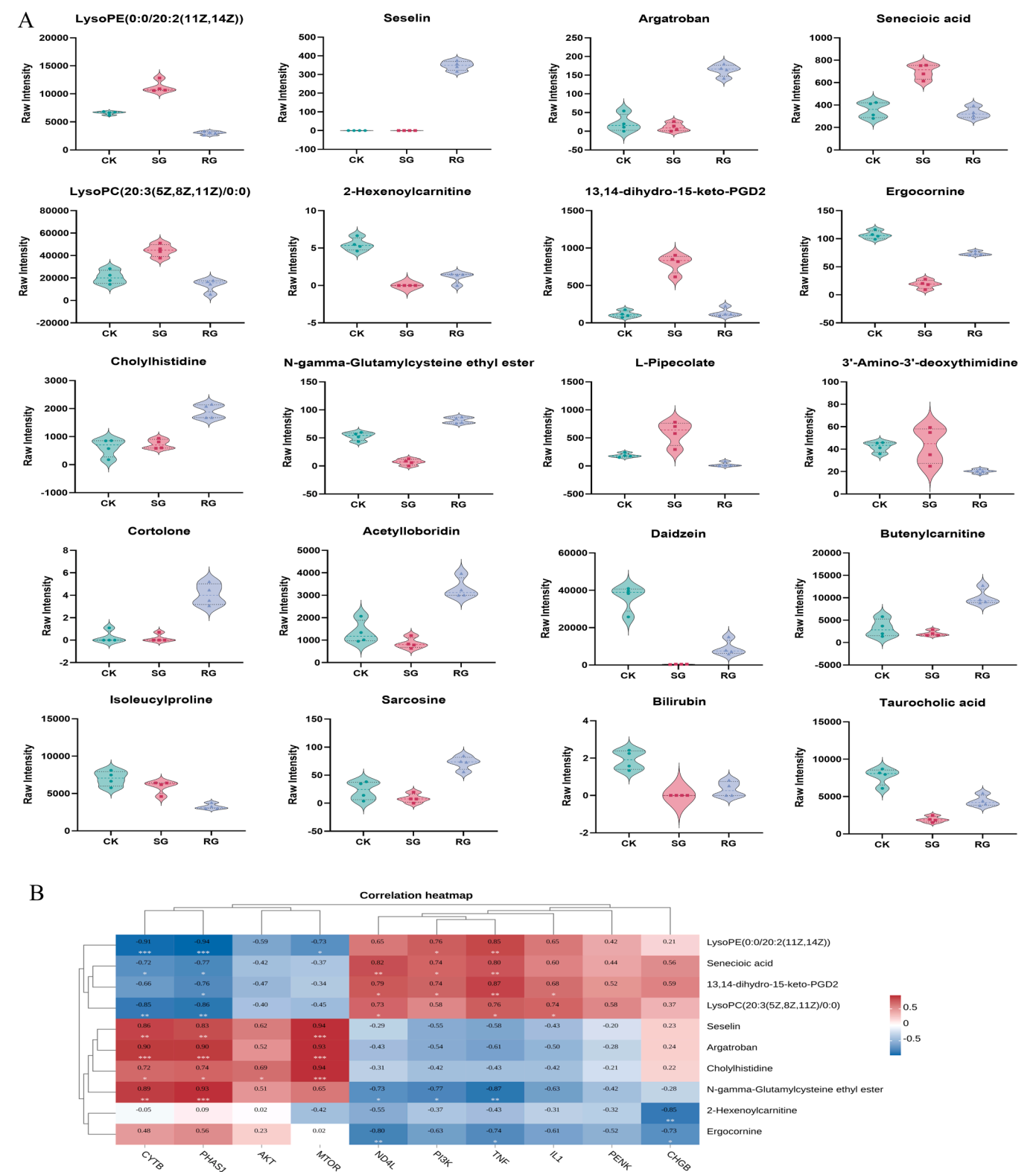


Fig. 6. Serum metabolic profile before and after molting. A, the distribution of the top 20 metabolites with the most significant differences in the three groups; B, for the cluster hot soil jointly analyzed by the top 20 differential metabolites and the top 10 differential genes, ** indicates significant difference, red represents positive correlation, and blue represents negative correlation.

ovarian development of molting laying hens.

Conclusion

Forced molting has been demonstrated to improve the serum

metabolic profile of laying hens, modulate the PI3K-AKT-mTOR signaling pathway, and subsequently activate the expression of Ki-67 and PHAS1 proteins. These alterations promote ovarian development and contribute to an increase in egg production. This research provides a theoretical foundation for advancements in layer breeding and the

optimization of egg production.

CRediT authorship contribution statement

Mengqing Sun: Visualization, Investigation, Data curation. **Hailing Wang:** Visualization, Investigation. **Xinyu Zhu:** Data curation. **Xiaohan Zhang:** Conceptualization. **Yahong Min:** Visualization. **Ming Ge:** Methodology. **Xiaowen Jiang:** Visualization. **Wenhui Yu:** Methodology, Investigation, Data curation.

Declaration of competing interest

The authors have no conflicts of interest to declare.

Acknowledgments

This research was supported by the National Key Research and Development Program of China (Grant No. 2017YFD0502200).

Supplementary materials

Supplementary material associated with this article can be found, in the online version, at [doi:10.1016/j.psj.2025.105125](https://doi.org/10.1016/j.psj.2025.105125).

References

- Aloodan, M.A., Mashaly, M.M., 1999. Effect of induced molting in laying hens on production and immune parameters. *Poult. Sci.* 78, 171–177. <https://doi.org/10.1093/ps/78.2.171>.
- Attia, Y.A., Burke, W.H., Yamani, K.A., 1994. Response of broiler breeder hens to forced molting by hormonal and dietary manipulations. *Poult. Sci.* 73, 245–258. <https://doi.org/10.3382/ps.0730245>.
- Berry, W.D., 2003. The physiology of induced molting. *Poult. Sci.* 82, 971–980. <https://doi.org/10.1093/ps/82.6.971>.
- Borrell-Pages, M., Luquero, A., Vilahur, G., Padró, T., Badimon, L., 2024. Canonical wnt pathway and the LDL receptor superfamily in neuronal cholesterol homeostasis and function. *Cardiovasc. Res.* 120, 140–151. <https://doi.org/10.1093/cvr/cvad159>.
- Bozkurt, M., Bintaş, E., Kırkan, Ş., Akşit, H., Küçükyılmaz, K., Erbaş, G., Çabuk, M., Akşit, D., Parın, U., Ege, G., Koçer, B., Seyrek, K., Tüzün, A.E., 2016. Comparative evaluation of dietary supplementation with mannan oligosaccharide and oregano essential oil in forced molted and fully fed laying hens between 82 and 106 weeks of age. *Poult. Sci.* 95, 2576–2591. <https://doi.org/10.3382/ps/pew140>.
- Brieno-Enríquez, M.A., Faykoo-Martinez, M., Gobon, M., Grenier, J.K., McGrath, A., Prado, A.M., Sinopoli, J., Wagner, K., Walsh, P.T., Lopa, S.H., Laird, D.J., Cohen, P. E., Wilson, M.D., Holmes, M.M., Place, N.J., 2023. Postnatal oogenesis leads to an exceptionally large ovarian reserve in naked mole-rats. *Nat. Commun.* 14, 670. <https://doi.org/10.1038/s41467-023-36284-8>.
- Brunn, G.J., Williams, J., Sabers, C., Wiederricht, G., Lawrence Jr., J.C., Abraham, R.T., 1996. Direct inhibition of the signaling functions of the mammalian target of rapamycin by the phosphoinositide 3-kinase inhibitors, wortmannin and LY294002. *EMBO J.* 15, 5256–5267.
- Chen, G., Goeddel, D.V., 2002. TNF-R1 signaling: a beautiful pathway. *Science* 296, 1634–1635. <https://doi.org/10.1126/science.1071924>.
- Chen, X., Chen, W., Ci, W., Zheng, Y., Han, X., Huang, J., Zhu, J., 2023. Effects of dietary supplementation with *Lactobacillus acidophilus* and *Bacillus subtilis* on mucosal immunity and intestinal barrier are associated with its modulation of gut metabolites and microbiota in late-phase laying hens. *Probiot. Antimicrob. Proteins* 15 (4), 912–924. <https://doi.org/10.1007/s12602-022-09923-7>.
- Cheng, H., Wei, F., Del Valle, J.S., Stolk, T.H.R., Huirne, J.A., Asseler, J.D., Pilgram, G.S. K., Van Der Westerlaken, L.A.J., Van Mello, N.M., Chuva De Sousa Lopes, S.M., 2024. In vitro growth of secondary follicles from cryopreserved-thawed ovarian cortex. *Hum. Reprod. (Oxf. Engl.)* 39, 2743–2753. <https://doi.org/10.1093/humrep/deae240>.
- Cheng, J., Huang, Y., Zhang, X., Yu, Y., Wu, S., Jiao, J., Tran, L., Zhang, W., Liu, R., Zhang, L., Wang, M., Wang, M., Yan, W., Wu, Y., Chi, F., Jiang, P., Zhang, X., Wu, H., 2020. TRIM21 and PHLD3 negatively regulate the crosstalk between the PI3K/AKT pathway and PPP metabolism. *Nat. Commun.* 11, 1880. <https://doi.org/10.1038/s41467-020-15819-3>.
- Chidambaram, S., El-Sheikh, M.A., Alfarhan, A.H., Radhakrishnan, S., Akbar, I., 2021. Synthesis of novel coumarin analogues: investigation of molecular docking interaction of SARS-CoV-2 proteins with natural and synthetic coumarin analogues and their pharmacokinetics studies. *Saudi J. Biol. Sci.* 28, 1100–1108. <https://doi.org/10.1016/j.sjbs.2020.11.038>.
- Contina, A., Bossu, C.M., Allen, D., Wunder, M.B., Ruegg, K.C., 2023. Genetic and ecological drivers of molt in a migratory bird. *Sci. Rep.* 13, 814. <https://doi.org/10.1038/s41598-022-26973-7>.
- Corrier, D.E., Nisbet, D.J., Hargis, B.M., Holt, P.S., DeLoach, J.R., 1997. Provision of lactose to molting hens enhances resistance to *Salmonella enteritidis* colonization. *J. Food Prot.* 60, 10–15. <https://doi.org/10.4315/0362-028X-60.1.10>.
- Elsagheer, M.A., Mohamed, O.A., Khattab, I.M., Wade, M.K., 2024. Impact of different mating ratios of broiler breeder on reproductive performance during post moult phase. *Anim. Biotechnol.* 35 (1), 2398707. <https://doi.org/10.1080/10495398.2024.2398707>.
- Gao, Z., Gao, X., Fan, W., Liu, S., Li, M., Miao, Y., Ding, C., Tang, Z., Yan, L., Liu, G., Shi, X., Song, S., 2021. Bisphenol A and genistein have opposite effects on adult chicken ovary by acting on *erα*/Nrf2-Keap1-signaling pathway. *Chem. Biol. Interact.* 347, 109616. <https://doi.org/10.1016/j.cbi.2021.109616>.
- Ge, Y., Lin, S., Li, B., Yang, Y., Tang, X., Shi, Y., Sun, J., Le, G., 2020. Oxidized pork induces oxidative stress and inflammation by altering gut microbiota in mice. *Mol. Nutr. Food Res.* 64 (2), e1901012. <https://doi.org/10.1002/mnfr.201901012>.
- Greger, H., Zechner, G., Hofer, O., Vajrodaya, S., 1996. Bioactive amides from *Glycosmis* species. *J. Nat. Prod.* 59, 1163–1168. <https://doi.org/10.1021/np9604238>.
- Gu, Y.F., Chen, Y.P., Jin, R., Wang, C., Wen, C., Zhou, Y.M., 2021. Age-related changes in liver metabolism and antioxidant capacity of laying hens. *Poult. Sci.* 100, 101478. <https://doi.org/10.1016/j.psj.2021.101478>.
- Ha, C.Y., Kim, J.-Y., Paik, J.K., Kim, O.Y., Paik, Y.H., Lee, E.J., Lee, J.H., 2012. The association of specific metabolites of lipid metabolism with markers of oxidative stress, inflammation and arterial stiffness in men with newly diagnosed type 2 diabetes. *Clin. Endocrinol.* 76 (5), 674–682. <https://doi.org/10.1111/j.1365-2265.2011.04244.x>.
- Herremans, M., 1988. Age and strain differences in plumage renewal during natural and induced molting in hybrid hens. *Br. Poult. Sci.* 29, 825–835. <https://doi.org/10.1080/00071668808417111>.
- Heryanto, B., Yoshimura, Y., Tamura, T., 1997. Cell proliferation in the process of oviductal tissue remodeling during induced molting in hens. *Poult. Sci.* 76, 1580–1586. <https://doi.org/10.1093/ps/76.11.1580>.
- Hu, H., Huang, Y., Li, A., Mi, Q., Wang, K., Chen, L., Zhao, Z., Zhang, Q., Bai, X., Pan, H., 2024. Effects of different energy levels in low-protein diet on liver lipid metabolism in the late-phase laying hens through the gut-liver axis. *J. Anim. Sci. Biotechnol.* 15, 98. <https://doi.org/10.1186/s40104-024-01055-y>.
- Huang, J., Hu, Y., Tong, X., Zhang, L., Yu, Z., Zhou, Z., 2020. Untargeted metabolomics revealed therapeutic mechanisms of icariin on low bone mineral density in older caged laying hens. *Food Funct.* 11, 3201–3212. <https://doi.org/10.1039/c9fo02882j>.
- Huo, S., Li, Y., Guo, Y., Zhang, S., Li, P., Gao, P., 2020. Improving effects of epimedii flavonoids on the selected reproductive features in layer hens after forced molting. *Poult. Sci.* 99, 2757–2765. <https://doi.org/10.1016/j.psj.2019.12.053>.
- Jenni, L., Ganz, K., Milanese, P., Winkler, R., 2020. Determinants and constraints of feather growth. *PLoS One* 15, e0231925. <https://doi.org/10.1371/journal.pone.0231925>.
- Kim, D.H., Lee, Y.-K., Lee, S.D., Lee, K.W., 2022. Impact of relative humidity on the laying performance, egg quality, and physiological stress responses of laying hens exposed to high ambient temperature. *J. Therm. Biol.* 103, 103167. <https://doi.org/10.1016/j.jtherbio.2021.103167>.
- Korver, D.R., 2023. Review: current challenges in poultry nutrition, health, and welfare. *Anim. Int. J. Anim. Biosci.* 17 (2), 100755. <https://doi.org/10.1016/j.animal.2023.100755>. Suppl.
- Kumar, R., Hegde, A.S., Sharma, K., Parmar, P., Srivatsan, V., 2022. Microalgae as a sustainable source of edible proteins and bioactive peptides - current trends and future prospects. *Food Res. Int.* 157, 111338. <https://doi.org/10.1016/j.foodres.2022.111338>.
- Landers, K.L., Moore, R.W., Dunkley, C.S., Herrera, P., Kim, W.K., Landers, D.A., Howard, Z.R., McReynolds, J.L., Bryd, J.A., Kubena, L.F., Nisbet, D.J., Ricke, S.C., 2008. Immunological cell and serum metabolite response of 60-week-old commercial laying hens to an alfalfa meal molt diet. *Bioresour. Technol.* 99, 604–608. <https://doi.org/10.1016/j.biortech.2006.12.036>.
- Len, R.E., Abplanalp, H., Johnson, E.A., 1964. Second year production of force molted hens in the California random sample test. *Poult. Sci.* 43 (3), 638–646. <https://doi.org/10.3382/ps.0430638>.
- Li, H., Wang, R., 2017. Blocking SIRT1 inhibits cell proliferation and promotes aging through the PI3K/AKT pathway. *Life Sci.* 190, 84–90. <https://doi.org/10.1016/j.lfs.2017.09.037>.
- Li, P., Zhao, Y., Yan, S., Song, B., Liu, Y., Gao, M., Tang, D., Guo, Y., 2022. Soya saponin improves egg-laying performance and immune function of laying hens. *J. Anim. Sci. Biotechnol.* 12, 126. <https://doi.org/10.1186/s40104-021-00647-2>.
- Lim, C.I., Ryu, K.S., 2022. Effect of dietary octacosanol concentration extracted from triticale sprout on laying performance, egg quality, and blood parameters of laying hens. *J. Anim. Sci. Technol.* 64, 863–870. <https://doi.org/10.5187/jast.2022.e62>.
- Liu, M., Kang, Z., Cao, X., Jiao, H., Wang, X., Zhao, J., Lin, H., 2024. Prevotella and succinate treatments altered gut microbiota, increased laying performance, and suppressed hepatic lipid accumulation in laying hens. *J. Anim. Sci. Biotechnol.* 15, 26. <https://doi.org/10.1186/s40104-023-00975-5>.
- Lu, J., Mitra, S., Wang, X., Khaidakov, M., Mehta, J.L., 2011. Oxidative stress and lectin-like ox-LDL-receptor LOX-1 in atherosclerosis and tumorigenesis. *Antioxid. Redox Signal.* 15, 2301–2333. <https://doi.org/10.1089/ars.2010.3792>.
- McKeage, K., Plosker, G.L., 2001. Argatroban. *Drugs* 61, 515–522. <https://doi.org/10.2165/00003495-200161040-00005> discussion 523–514.
- Mishra, R., Mishra, B., Kim, Y.S., Jha, R., 2022. Practices and issues of molting programs for laying hens: a review. *Br. Poult. Sci.* 63, 720–729. <https://doi.org/10.1080/00071668.2022.2059339>.
- Nii, T., Sonoda, Y., Isobe, N., Yoshimura, Y., 2011. Effects of lipopolysaccharide on the expression of proinflammatory cytokines and chemokines and the subsequent

- recruitment of immunocompetent cells in the oviduct of laying and molting hens. *Poult. Sci.* 90, 2332–2341. <https://doi.org/10.3382/ps.2011-01596>.
- Nishiyama, T., Nakagawa, K., Imabayashi, T., Iwatani, S., Yamamoto, N., Tsushima, N., 2021. Probiotic *Bacillus subtilis* C-3102 improves eggshell quality after forced molting in aged laying hens. *J. Poult. Sci.* 58, 230–237. <https://doi.org/10.2141/jpsa.0200081>.
- Perry, M.M., Griffin, H.D., Gilbert, A.B., 1984. The binding of very low density and low density lipoproteins to the plasma membrane of the hen's oocyte. A morphological study. *Exp. Cell Res.* 151, 433–446. [https://doi.org/10.1016/0014-4827\(84\)90393-8](https://doi.org/10.1016/0014-4827(84)90393-8).
- Qiang, T., Wang, J., Ding, X., Zeng, Q., Bai, S., Lv, L., Xuan, Y., Peng, H., Zhang, K., 2023. The improving effect of soybean isoflavones on ovarian function in older laying hens. *Poult. Sci.* 102, 102944. <https://doi.org/10.1016/j.psj.2023.102944>.
- Ragupathi, A., Kim, C., Jacinto, E., 2024. The mTORC2 signaling network: targets and cross-talks. *Biochem. J.* 481, 45–91. <https://doi.org/10.1042/bcj20220325>.
- Ritsick, D.R., Edens, W.A., Finnerty, V., Lambeth, J.D., 2007. Nox regulation of smooth muscle contraction. *Free Radic. Biol. Med.* 43, 31–38. <https://doi.org/10.1016/j.freeradbiomed.2007.03.006>.
- Roh, C., Han, J., Tzatsos, A., Kandror, K.V., 2003. Nutrient-sensing mTOR-mediated pathway regulates leptin production in isolated rat adipocytes. *Am. J. Physiol. Endocrinol. Metab.* 284, E322. <https://doi.org/10.1152/ajpendo.00230.2002>.
- Ruan, Z.R., Yu, Z., Xing, C., Chen, E.H., 2024. Inter-organ steroid hormone signaling promotes myoblast fusion via direct transcriptional regulation of a single key effector gene. *Curr. Biol.* 34, 1438–1452. <https://doi.org/10.1016/j.cub.2024.02.056>.
- Schmitz, J., Owyang, A., Oldham, E., Song, Y., Murphy, E., McClanahan, T.K., Zurawski, G., Moshrefi, M., Qin, J., Li, X., Gorman, D.M., Bazan, J.F., Kastelein, R.A., 2005. IL-33, an interleukin-1-like cytokine that signals via the IL-1 receptor-related protein ST2 and induces T helper type 2-associated cytokines. *Immunity* 23, 479–490. <https://doi.org/10.1016/j.immuni.2005.09.015>.
- She, Q.B., Solit, D.B., Ye, Q., O'Reilly, K.E., Lobo, J., Rosen, N., 2005. The BAD protein integrates survival signaling by EGFR/MAPK and PI3K/akt kinase pathways in PTEN-deficient tumor cells. *Cancer Cell* 8, 287–297. <https://doi.org/10.1016/j.ccr.2005.09.006>.
- Soares, J.R.P., Dos Santos, C.C., 2025. Effect of naringenin and senecioic acid ester derivatives on astrocyte antioxidant mechanism and reactivity after inflammatory stimulus. *Int. J. Mol. Sci.* 26, 2215. <https://doi.org/10.3390/ijms26052215>.
- Sun, X., Chen, X., Zhao, J., Ma, C., Yan, C., Liswaniso, S., Xu, R., Qin, N., 2021. Transcriptome comparative analysis of ovarian follicles reveals the key genes and signaling pathways implicated in hen egg production. *BMC Genom.* 22, 899. <https://doi.org/10.1186/s12864-021-08213-w>.
- Sundaresan, N.R., Anish, D., Sastry, K.V., Saxena, V.K., Mohan, J., Saxena, M., 2007. Differential expression of lipopolysaccharide-induced TNF-alpha factor (LITAF) in reproductive tissues during induced molting of white leghorn hens. *Anim. Reprod. Sci.* 102, 335–342. <https://doi.org/10.1016/j.anireprosci.2007.01.022>.
- Sundaresan, N.R., Anish, D., Sastry, K.V., Saxena, V.K., Nagarajan, K., Subramani, J., Leo, M.D., Shit, N., Mohan, J., Saxena, M., Ahmed, K.A., 2008. High doses of dietary zinc induce cytokines, chemokines, and apoptosis in reproductive tissues during regression. *Cell Tissue Res.* 332, 543–554. <https://doi.org/10.1007/s00441-008-0599-3>.
- Surai, P.F., Fisinin, V.I., 2014. Selenium in poultry breeder nutrition: an update. *Anim. Feed Sci. Technol.* 191, 1–15. <https://doi.org/10.1016/j.anifeedsci.2014.02.005>.
- Tang, Y., Yin, L., Liu, L., Chen, Q., Lin, Z., Zhang, D., Wang, Y., Liu, Y., 2023. Comparative analysis of different proteins and metabolites in the liver and ovary of local breeds of chicken and commercial chickens in the later laying period. *Int. J. Mol. Sci.* 24 (18), 14394. <https://doi.org/10.3390/ijms241814394>.
- Tian, W.H., Wang, Z., Yue, Y.X., Li, H., Li, Z.J., Han, R.L., Tian, Y.D., Kang, X.T., Liu, X. J., 2019. miR-34a-5p increases hepatic triglycerides and total cholesterol levels by regulating ACSL1 protein expression in laying hens. *Int. J. Mol. Sci.* 20 (18), 4420. <https://doi.org/10.3390/ijms20184420>.
- Wang, C., Sun, X., Liu, X., Wang, Y., Luo, J., Yang, X., Liu, Y., 2024. Protective effects of betaine on the early fatty liver in laying hens through ameliorating lipid metabolism and oxidative stress. *Front. Nutr.* 11, 1505357. <https://doi.org/10.3389/fnut.2024.1505357>.
- Wang, H., Cahaner, A., Lou, L., Zhang, L., Ge, Y., Li, Q., Zhang, X., 2022. Genetics and breeding of a black-bone and blue eggshell chicken line. 2. Laying patterns and egg production in two consecutive generations. *Poult. Sci.* 101, 101679. <https://doi.org/10.1016/j.psj.2021.101679>.
- Wein, Y., Shira, E.B., Friedman, A., 2020. Increased serum levels of advanced glycation end products due to induced molting in hen layers trigger a proinflammatory response by peripheral blood leukocytes. *Poult. Sci.* 99, 3452–3462. <https://doi.org/10.1016/j.psj.2020.04.009>.
- Widelitz, R.B., Lin, G.W., Lai, Y.C., Mayer, J.A., Tang, P.C., Cheng, H.C., Jiang, T.X., Chen, C.F., Chuong, C.M., 2019. Morpho-regulation in diverse chicken feather formation: integrating branching modules and sex hormone-dependent morpho-regulatory modules. *Dev. Growth Differ.* 61, 124–138. <https://doi.org/10.1111/dgd.12584>.
- Wu, X.L., Zou, X.Y., Zhang, M., Hu, H.Q., Wei, X.L., Jin, M.L., Cheng, H.W., Jiang, S., 2021. Osteocalcin prevents insulin resistance, hepatic inflammation, and activates autophagy associated with high-fat diet-induced fatty liver hemorrhagic syndrome in aged laying hens. *Poult. Sci.* 100, 73–83. <https://doi.org/10.1016/j.psj.2020.10.022>.
- Xiang, X., Huang, X., Wang, J., Zhang, H., Zhou, W., Xu, C., Huang, Y., Tan, Y., Yin, Z., 2022. Transcriptome analysis of the ovaries of Taihe black-bone silky fowls at different egg-laying stages. *Genes (Basel)* 13 (11), 2066. <https://doi.org/10.3390/genes13112066>.
- Xie, X., Hu, H., Tong, X., Li, L., Liu, X., Chen, M., Yuan, H., Xie, X., Li, Q., Zhang, Y., Ouyang, H., Wei, M., Huang, J., Liu, P., Gan, W., Liu, Y., Xie, A., Kuai, X., Chirn, G. W., Zhou, H., Zeng, R., Hu, R., Qin, J., Meng, F.L., Wei, W., Ji, H., Gao, D., 2018. The mTOR-S6K pathway links growth signalling to DNA damage response by targeting RNF168. *Nat. Cell Biol.* 20, 320–331. <https://doi.org/10.1038/s41556-017-0033-8>.
- Xing, L., Zhang, R., Gong, R., Liu, X., Bao, J., Li, J., 2022. Ameliorative effects of dietary selenium against cadmium toxicity on production performance and egg quality in laying hens. *Ecotoxicol. Env. Saf.* 248, 114317. <https://doi.org/10.1016/j.ecoenv.2022.114317>.
- Yan, P., Liu, J., Huang, Y., Li, Y., Yu, J., Xia, J., Liu, M., Bai, R., Wang, N., Guo, L., Liu, G., Yang, X., Zeng, J., He, B., 2023. Lotus leaf extract can attenuate salpingitis in laying hens by inhibiting apoptosis. *Poult. Sci.* 102, 102865. <https://doi.org/10.1016/j.psj.2023.102865>.
- Yang, B., Huang, S., Zhao, G., Ma, Q., 2022. Dietary supplementation of porcine bile acids improves laying performance, serum lipid metabolism and cecal microbiota in late-phase laying hens. *Anim. Nutr. (Zhongguo xu mu shou yi xue hui)* 11, 283–292. <https://doi.org/10.1016/j.aninu.2022.08.003>.
- Zhang, J., Cui, J., Wang, Y., Lin, X., Teng, X., Tang, Y., 2022a. Complex molecular mechanism of ammonia-induced apoptosis in chicken peripheral blood lymphocytes: miR-27b-3p, heat shock proteins, immunosuppression, death receptor pathway, and mitochondrial pathway. *Ecotoxicol. Env. Saf.* 236, 113471. <https://doi.org/10.1016/j.ecoenv.2022.113471>.
- Zhang, T., Chen, Y., Wen, J., Jia, Y., Wang, L., Lv, X., Yang, W., Qu, C., Li, H., Wang, H., Qu, L., Ning, Z., 2021. Transcriptomic analysis of laying hens revealed the role of aging-related genes during forced molting. *Genes (Basel)* 12 (11), 1767. <https://doi.org/10.3390/genes12111767>.
- Zhang, Y., Meng, J., Zhang, L., Bao, J., Shi, W., Li, Q., Wang, X., 2022b. Shudi Erzi San relieves ovary aging in laying hens. *Poult. Sci.* 101, 102033. <https://doi.org/10.1016/j.psj.2022.102033>.
- Zhao, C., Zhou, T., Zhao, X., Pang, Y., Li, W., Fan, B., Li, M., Liu, X., Ma, L., Zhang, J., Sun, C., Shen, W., Kong, X., Yao, X., Feng, S., 2022. Delayed administration of nafamostat mesylate inhibits thrombin-mediated blood-spinal cord barrier breakdown during acute spinal cord injury in rats. *J. Neuroinflammation* 19, 189. <https://doi.org/10.1186/s12974-022-02531-w>.
- Zhu, M., Miao, S., Zhou, W., Elnesr, S.S., Dong, X., Zou, X., 2021. MAPK, AKT/FoxO3a and mTOR pathways are involved in cadmium regulating the cell cycle, proliferation and apoptosis of chicken follicular granulosa cells. *Ecotoxicol. Env. Saf.* 214, 112091. <https://doi.org/10.1016/j.ecoenv.2021.112091>.
- Zimova, M., Hackländer, K., Good, J.M., Melo-Ferreira, J., Alves, P.C., Mills, L.S., 2018. Function and underlying mechanisms of seasonal colour moulting in mammals and birds: what keeps them changing in a warming world? *Biol. rev. Camb. Philos. Soc.* 93, 1478–1498. <https://doi.org/10.1111/brv.12405>.